CHALLENGES IN DEVELOPING A SOLAR POWERED STIRLING ENGINE FOR DOMESTIC ELECTRICITY GENERATION

R. Mangion[*#], M. Muscat[*], T. Sant[*], J.Rizzo[#], R. Ghirlando[*], J. Cilia[+], J. Mizzi[+#], S. Vural[#]

[*]Department of Mechanical Engineering, University of Malta, Malta
[+]Department of Industrial Electrical Power Conversion, University of Malta, Malta
[#]SIRIUS systems Ltd., Lija, Malta

ABSTRACT

This paper investigates the challenges in developing a solar powered Stirling engine for domestic electricity generation. All the system components, the parabolic troughs, heat transfer fluid and the Stirling engine are individually analysed. The analysis includes a market survey and performance assessments of such components. A mathematical analysis for the Stirling engine is carried out in order to understand the affect of varies parameters with the work output per cycle and the engine efficiency. Such parameters are the phase angle between pistons, the diameter ratio of the power and displacer piston, and change in temperature.

NOMENCLATURE

Be	[-]	Beale number
c_v	[J/kgK]	Specific heat capacity at constant volume
c_p	[J/kgK]	Specific heat capacity at constant pressure
f	[Hz]	Frequency
D	[m]	Diameter
M	[kg]	Total mass
m	[kg]	Instantaneous mass
p	[Pa]	Pressure
P	[W]	Power
Q	[-]	Heat energy
R	[J/kgK]	Specific gas constant
T	[K]	Temperature
ΔT	[°C]	Temperature difference
V	[m³]	Volume
ΔV	[m³]	Change in volume (swept volume by power piston)
V_{OL}	[m³]	Overlapped volume
W	[J]	Work

Greek letters

α	[°]	Phase angle between displacer and power piston
γ	[-]	Volumetric expansivity
ε	[-]	Compression ratio
θ	[°]	Crank angle
η	[-]	Efficiency

Subscripts

c	Compression
C	Carnot
D	Displacer
e	Expansion
h	Heater
k	Cooler
max	Maximum
min	Minimum
p	Power piston
r	Regenerator
s	Stirling

INTRODUCTION

Nowadays the use of renewable energy sources is rapidly increasing in its importance. This is mainly due to the fact that certain countries are now bound by legislation to reduce carbon emissions and reduce their dependency on fossil fuels. For example member states of the European Union are bound by EU directives which specify the percentage amount of the final energy consumption that should be produced from renewable sources by the end of 2020.

Small countries such as Malta, have limited open area at ground level that can accommodate large grid connected concentrated solar power or large photovoltaic systems. However, considerable space exists on domestic and industrial roof tops. In Malta most buildings have flat roof tops making them quite versatile for installation of these renewable energy systems. The current trend is to cover these roof top areas with photovoltaic panels. This is due to the photovoltaic panels' reliability and reasonable efficiency. Although photovoltaic panels are commercially available at relatively reasonable prices, it is interesting to test the undiscovered potential of micro-scale concentrated solar power heat engines.

Solar-powered Stirling engines can potentially be alternative candidates for micro-scale solar systems for domestic use. Currently, Stirling engines are mainly powered by concentrating solar energy at the focal point of paraboloidal dishes. For these systems the minimum size of the dish is about 3.75m in diameter. This size of dish is quite prohibitive to be installed on a domestic rooftop. Problems that can be encountered include wind loading, aesthetics and acquiring local planning permits for such installations.

This paper describes the proposed development of a system utilising parabolic troughs as energy collectors. A heat transfer fluid passes through the receivers which are located in the troughs' focal line. The energy absorbed by the heat transfer fluid is then used as a heat source for the Stirling engine. There are a number of advantages for such a system. One of these advantages is that the size of parabolic troughs is quite similar to that of photovoltaic panels. Therefore they are less subjected to wind loading and are aesthetically more pleasing. Another advantage of such systems is the potential for energy storage to cover periods of indirect sunlight.

The major challenge of the proposed micro scale concentrated solar power system is the relatively low temperature (250-350°C) that can currently be reached by

small aperture parabolic troughs. Thus, a Stirling engine which gives a reasonable power output and efficiency at this temperature range has to be developed. Nearly all Stirling engines available on the market operate at a temperature higher than 650°C [1]. Moreover, in order to be competitive, the efficiency and cost of the complete system has to be at least the same level as the photovolatic panels.

PHOTOVOLTAIC (PV) SYSTEMS AVAILABLE ON THE MARKET

A PV system consists of a number of PV modules where each module consists of a number of solar cells, when incident solar radiation shines on a solar cell, the photon is absorbed and electron-hole pairs are generated. This will generate a flow of direct current that is fed to an inverter, where this is converted into alternating current and consequently consumed or fed into the grid.

The three main types of PV module technologies amongst the various available are monocrystalline silicon, polycrystalline silicon and thin film. The main differences between the performance is that the efficiency of the monocrystalline and the polycrystalline decreases as the temperature of the panel increases while the efficiency of thin film remains fairly stable. On the other hand the efficiency of monocrystalline and the polycrystalline is approximately 2.5 times higher than that of thin film, making them the most suitable technologies when the area available is limited. The output of a PV system decreases with the age of the system. From the technologies available today one should expect the output to reduce to 90% after 10 years of operation and to 80% after 25 years of operation.

PV systems are still limited in their efficiency and although their reasonable price, they are still quite expensive to compete with conventional electricity generation. Furthermore PV systems are negatively affected when they are in shade since their output drops rapidly. Thus, a micro scale solar power Stirling engine system may result in a better solution in terms of cost and efficiency.

STIRLING ENGINE CHALLENGES

A Stirling engine is a heat engine that subjects the working fluid to a closed loop cycle. An external heat source is used to supply heat to the engine. This results in a relatively silent engine in comparison with IC engine since no explosive combustion is occurring. Another advantage of the Stirling engine is that less 'toxic' exhaust is emitted by the engine. Furthermore the Stirling engine requires low maintenance and creates minimal vibrations. This gives it the potential to be installed on roof tops.

Market availability

Studies were conducted to analyse what Stirling engines are available on the market and whether they operate at the required temperature i.e. 250-350°C reached by small aperture parabolic solar troughs. In these studies the authors were analysing engines that deliver 3kW of shaft power or less. From this investigation it was concluded that the majority of the existing engines are prototypes and few are 'commercially'

available. Furthermore the majority of the engines surveyed operate at a temperature above 500°C.

The engines surveyed were developed by: Genoa Stirling, which has a variety of 3 engines ranging from 350W, 1kW and 3kW and working temperature of 750°C [2]; Sun Power, who offer a 1kW free piston engine [3]; Whispergen, offer a 1 kW kinematic Stirling engine which is used in micro combined heat and power unit [4]; Infina who offer two engines (1kW and a 3kW) both free piston [5] and Microgen who developed a 1kW free piston engine. [6] Only one engine was found to operate at temperature below 300°C. This latter engine is still in the testing phase and is being developed by Cool Energy [7].

Due to the lack of engine availability operating at low/medium temperature, it is clear that such an engine is still relatively underdeveloped.

Thermodynamics of the Stirling engine

The thermodynamic cycle of a Stirling engine is illustrated in Figure 1. It consists of two constant volume processes and two isothermal processes. Heat is supplied to the working fluid as the fluid expands isothermally from point 3 to point 4 at a fixed temperature. The rejection of heat occurs during the process from point 1 to point 2 where the fluid is compressed isothermally at the lowest temperature of the cycle. The two reversible constant volume processes (i.e. process 4 to 1 and process 2 to 3) connect the two isothermals. The rejected heat during process 4 to 1 is used as a heat input to the fluid during process 2 to 3. Assuming that this phenomenon is ideal and reversible the cycle may be said to operate at the Carnot efficiency. In order to achieve the Stirling cycle, a 100% efficient regenerator is required. The regenerator consists of a matrix/mesh of material which isolates the heat source from the heat sink, but at the same time allows the temperature to change gradually during the constant volume processes [8].
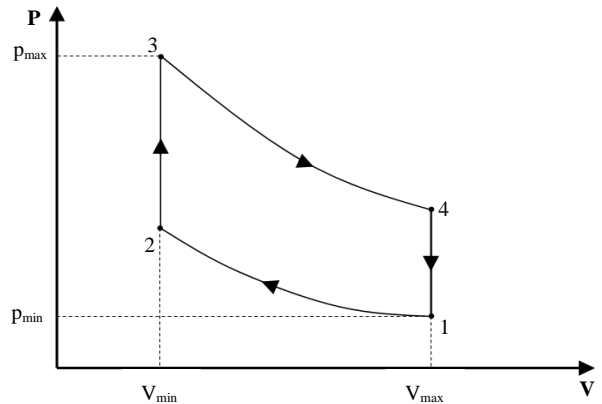

Figure 1 p-v diagram of an ideal Stirling engine

Engine configuration

Stirling engines are classified in three mechanical arrangements, alpha, beta and gamma. The alpha arrangement consists of two pistons placed in separate cylinders that are connected in series via a heater, regenerator and cooler. The beta and gamma arrangement consist of a displacer and a power piston. The displacer and the power piston in beta arrangement share the same cylinder while in the gamma arrangement they have separate cylinders [9] (Figure 2, [10]).

The main advantage of the alpha arrangement is the simple way in which it can be designed into a compact multiple cylinder which results in a high power output [9]. In case of beta arrangement the advantage is that it has minimal dead volume while the gamma configuration has rather large dead volumes which cause a reduction in power output [9].

The theoretical efficiency of a Stirling engine is that of the Carnot cycle, but in reality a well designed engine can reach between 40 to 70% of the Carnot efficiency [11].
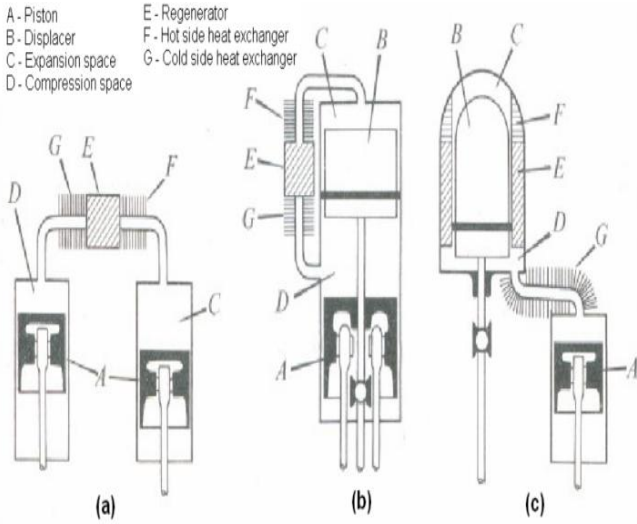
Figure 2 Stirling engine configurations ([10])
  a)   Alpha
  b)   Beta
  c)   Gamma

Developing a Stirling engine

In order to develop a low/medium Stirling engine, different analytical mathematical models can be used. Such models are going to be discussed in the coming section.

The expanded volume (ΔV) of the working fluid is directly dependent on the hot and cold, source and sink temperatures, Equation 1 describes this relationship.

$$\Delta V = \gamma V_{min} \Delta T \tag{1}$$

Related to the change in volume, is the compression ratio which is the ratio of the maximum volume to the minimum volume. According to Kolin [12], in the case of the Stirling engine it varies between 1 and 2, while Walker argues that the maximum compression ratio can reach 2.5 [11].

Trying to increase the compression ratio may result in having inadequate void volume in the heat exchanger. Thus, resulting in inadequate heat transfer surface area and/or high pressure drop due to excessive aerodynamics friction pressure [11]. The compression ratio is given by the following equation:

$$\varepsilon = \frac{V_{max}}{V_{min}} \tag{2}$$

$$\varepsilon = \frac{V_{min} + \Delta V}{V_{min}} \tag{3}$$

$$= 1 + \frac{\Delta V}{V_{min}} \tag{4}$$

Using Equations 1 and 4 results in:

$$\varepsilon = 1 + \gamma \Delta T \tag{5}$$

The compression ratio can also be equated to:

$$\varepsilon = 1 + \frac{1}{\left(\frac{V_{swept,D}}{V_{swept,p}}\right)} \tag{6}$$

Furthermore an empirical formula for compression ratio is given by Kolin [12]:

$$\varepsilon = 1 + \frac{\Delta T}{1100} \tag{7}$$

Where

$$V_{swept,D} = \frac{\pi D_D{}^2}{4} \cdot Stroke_D \tag{8}$$

and

$$V_{swept,P} = \frac{\pi D_P{}^2}{4} \cdot Stroke_p \tag{9}$$

The relationship between the compression ratio, ε, and the temperature difference between the heat source and sink, given in Equations 5 and 7 is illustrated in Figure 3. Figure 3 clearly shows that the empirical formula as given by Kolin [12] results in much lower compression ratio for a given temperature difference, than that calculated in theory.

The efficiency of the Stirling engine can be calculated by the Reitlinger theory [12]. The power for a given speed can be calculated by using various models. In this paper the 1st order model and the Beale method [11] are described in some detail in the subsequent sections.
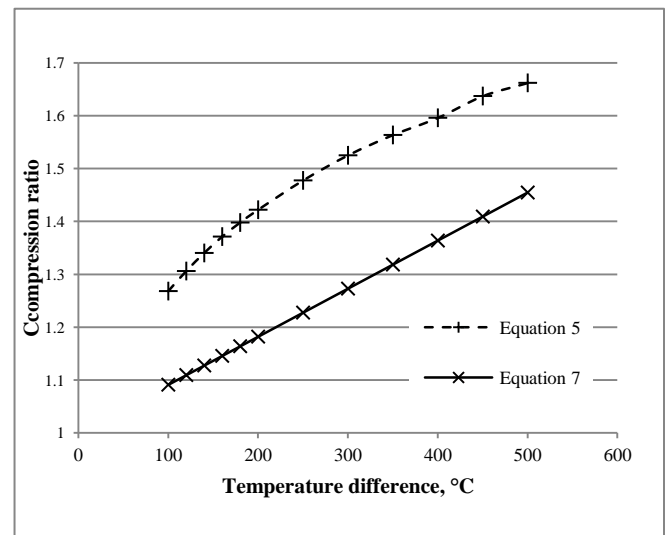
Figure 3 Compression ratio against temperature difference

Power and performance of the Stirling engine

Various mathematical models to predict the performance of a Stirling engine exist. Usually the most popular models are subdivided into three orders; the first, second and third orders.

The first order uses the Schmidt analysis in order to obtain initial sizing of the engine and includes experience factors to make up for the assumptions taken [13]. This analytical approach is used at a preliminary stage in the design since it incorporates several assumptions such as isothermal working space and ideal heat exchangers. The Beale analysis method is also a type of first order model used for preliminary engine design [14].

The second order model uses the Schmidt analysis, Finkelstein's Adiabatic model or Philips' semi-Adiabatic model, etc. but considers engine losses [14].

The third order model is more extensive and is based on numerical analyses. This latter model is the most accurate of the three [13].

The Schmidt Correlation:

In the work for this paper the first order model is used for the initial design of a model Stirling engine. Microsoft Excel ® (2007) was used to mathematically model relationships between the ratio of the displacer and power piston diameters (D_D/D_p), and phase angle (α) at different temperatures (ΔT) both against the work output per cycle. The Stirling engine efficiency was calculated using the Reitlinger theory. The Schimdt analysis is based on the isothermal model. Although it is the simplest model, it is very helpful during the development of a Stirling engine. Using this analysis a reasonable accuracy in predicting the output power is achieved (when including various losses) but it cannot predict the actual efficiency [9].

Assumptions considered in the Schmidt analysis:
a) The working fluid in the expansion space and the heater is at the upper source temperature, whereas the working fluid in the compression space and the cooler is at the lower sink temperature.
b) Volumes of the working space vary sinusoidal.
c) The expansion and compression processes are isothermal.
d) The heat exchangers and the regenerator are 100% effective.
e) There is no leakage of the working fluid i.e. constant mass.
f) The equations of state for a perfect gas apply.
g) The rotational speed of the engine is uniform.
h) Steady state is established.
i) The potential and kinetic energy of the working fluid are neglected.
j) No pressure drops occur along pipes and ducts.

The Stirling engine is modelled by having individual components connected in series, these components are, the compression space (c), the cooler (k), the regenerator (r), the heater (h) and the expansion space (e) (Figure 4 [15].) The components considered in this model are treated as a homogenous entity where 'm' is the mass of the working fluid, 'T' is the absolute temperature and 'V' is the absolute volume of air in each component. [9]
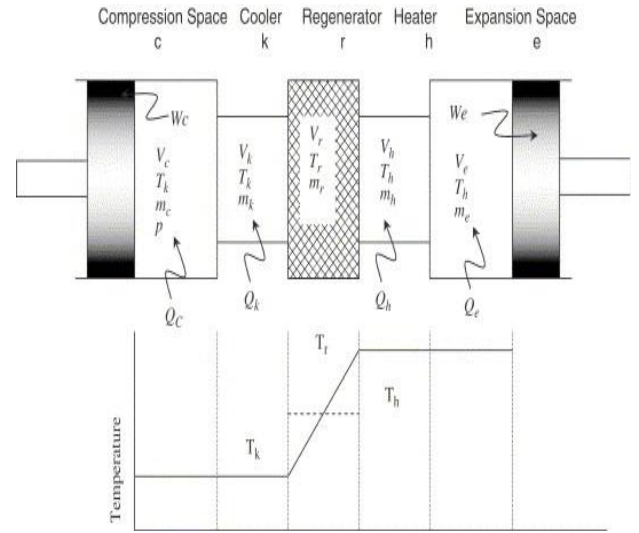

Figure 4 -Stirling engine model [15]

Over one complete cycle the work done is given by Equation 10 [13] [12]:

$$W = W_c + W_e = \oint p\,dV_c + \oint p\,dV_e$$
$$= p \oint \left(\frac{dV_c}{d\theta} + \frac{dV_e}{d\theta} \right) d\theta \tag{10}$$

Where

$$p = \frac{MRT}{V} \tag{11}$$

and

$$M = m_c + m_k + m_r + m_h + m_e \tag{12}$$

From Equation 11;

$$m = \frac{pV}{RT} \tag{13}$$

Hence

$$M = \frac{p}{R}\left(\left(\frac{V}{T}\right)_c + \left(\frac{V}{T}\right)_k + \left(\frac{V}{T}\right)_r + \left(\frac{V}{T}\right)_h + \left(\frac{V}{T}\right)_e \right) \tag{14}$$

Where T_r, temperature of the regenerator can be defined in various ways according to the analytical correlation used. It may be:

1. The log mean temperature [13](Walker correlation);

$$T_r = \frac{T_h - T_c}{\ln\left(\frac{T_h}{T_c}\right)} \tag{15}$$

2. The arithmetic mean [13] (Senft correlation);
3. T_r is at half volume hot, half volume cold [13] (Mayer Correlation);

$$T_r = \frac{1}{2}\left(\frac{1}{T_c} + \frac{1}{T_h} \right) \tag{16}$$

The expansion (hot) volume is given by [13]:

$$V_e = \frac{V_{swept,D,h}}{2}(1 - \cos\theta) + V_{unswept,D,h} \tag{17}$$

While the compression (cold) volume is given by [13]:

$$V_c = \frac{V_{swept,D,k}}{2}(1 + \cos\theta) + V_{unswept,D,k} \tag{18}$$

$$+ \frac{V_{swept,p}}{2}(1 - \cos(\theta - \alpha)) - V_{OL}$$

Where V_{OL} is the overlapped volume in the beta arrangement and is given by [13]:

$$V_{OL} = \frac{V_{swept,D,h} + V_{swept,p}}{2} \tag{19}$$

$$- \sqrt{\frac{V_{swept,D,h}{}^2 + V_{swept,p}{}^2}{4} - \frac{V_{swept,D,h} \cdot V_{swept,p}}{2} \cdot \cos\alpha}$$

In case of a gamma arrangement $V_{OL} = 0$

For an alpha arrangement [13];

$$V_e = \frac{V_{swept,h}}{2}(1 - \sin\theta) + V_{unswept,D,h} \tag{20}$$

$$V_c = \frac{V_{swept,k}}{2}(1 - \cos(\theta - \alpha)) + V_{unswept,D,k} \tag{21}$$

The work done can be evaluated by both analytical correlations and/or by numerically methods. When solving numerically it can be shown that when the crank angle (θ) increment is 0.25° there will be an error of 0.0003% in comparison with the analytical correlation developed by Mayers', Equation 22 [13]. Different analytical correlations similar to Mayers' i.e. Senft and Walker were developed according to the type of engine configuration.

The Mayer and Senft correlations used for beta and gamma arrangements are given by Equation 22 and Equation 28 respectively, while Walker correlation used for an alpha arrangement is given in Equation 36 [13].

Mayer correlation:

$$W = \frac{\pi \cdot MRT_k \cdot B \cdot V_{swept,p}}{B^2 + C^2}\left[\frac{A}{\sqrt{(A^2 - B^2 - C^2)}} - 1\right] \tag{22}$$

Where

$$A = X + \left(\frac{T_k}{T_h}\right)(Y) \tag{23}$$

$$X = \left(\frac{V_{swept,p}}{2} + V_{unswept,D,k} + \frac{V_{swept,D,k}}{2} + \frac{V_r}{2}\right) \tag{24}$$

$$Y = V_{unswept,D,h} + \frac{V_{swept,D,h}}{2} + \frac{V_r}{2} \tag{25}$$

$$B = \frac{V_{swept,D,h}}{2} \cdot \left(1 - \frac{T_k}{T_h}\right) \cdot \sin\alpha \tag{26}$$

$$C = \frac{1}{2}\left\{V_{swept,p} - \left[V_{swept,D,h}\left(1 - \frac{T_k}{T_h}\right) \cdot \cos\alpha\right]\right\} \tag{27}$$

Senft correlation:

$$W = \frac{\pi(1 - \tau)p_{max} \cdot V_{swept,D} \cdot k \cdot \sin\alpha}{Y + \sqrt{(Y^2 - X^2)}}\left[\frac{Y - X}{Y + X}\right]^{\frac{1}{2}} \tag{28}$$

Where

$$X = \sqrt{(\tau - 1)^2 + 2(\tau - 1)k \cdot \cos\alpha + k^2} \tag{29}$$

$$Y_{Beta} = \tau + \frac{4\chi\tau}{(1 + \tau)} + D \tag{30}$$

$$Y_{Gamma} = \tau + \frac{4\chi\tau}{(1 + \tau)} + 1 + k \tag{31}$$

$$D = \sqrt{(1 + k^2 - 2k \cdot \cos\alpha)} \tag{32}$$

$$\tau = \frac{T_k}{T_h} \tag{33}$$

$$\chi = \frac{V_{unswept,Total}}{V_{swept,D}} \tag{34}$$

$$k = \frac{V_{swept,p}}{V_{swept,D}} \tag{35}$$

Walker correlation:

In the case of an alpha arrangement, Walker gives the following a correlation;

$$W = p_{max} \cdot (1 + \kappa)V_{swept,e} \tag{36}$$

$$\cdot \pi\left(\frac{\tau - 1}{\kappa + 1}\right)\left(\frac{1 - \delta}{1 + \delta}\right)^{\frac{1}{2}}\left(\frac{\delta \sin\varphi}{1 + \sqrt{(1 - \delta^2)}}\right)$$

Where

$$\kappa = \frac{V_{swept,c}}{V_{swept,e}} \tag{37}$$

$$\delta = \frac{\sqrt{\tau^2 + 2\tau\kappa\cos\alpha + \kappa^2}}{\tau + \kappa + 2S} \tag{38}$$

$$S = \frac{2\left(\frac{V_{unswept,total}}{V_{swept,e}}\right)\tau}{\tau + 1} \tag{39}$$

$$\varphi = \tan^{-1}\left(\frac{\kappa \sin\alpha}{\tau + \kappa \cos\alpha}\right) \tag{40}$$

From the above analysis the power output can be calculated for a given R.P.M. The result can then be multiplied by experience factors such as those illustrated in Table 1 in order to achieve more realistic results [13].

Table 1 Power experience factors [13]

Author	Brake power to Calculated theoretical power
Urieli (1977)	$0.3 - 0.4$
Zarinchang (1975)	$0.3 - 0.4$
Finegold & Vanderbrug (1977)	0.32
Martini (1980)	0.6

Another method to establish the power output is by using the method developed by William Beale. This is based on experimental data available form various engines [9] the equation is as follows:

$$W = Be \cdot p_{mean} \cdot \Delta V \tag{41}$$

$$P = Be \cdot p_{mean} \cdot f \cdot \Delta V \tag{42}$$

The Beale number can be obtained from [14]

Efficiency of the Stirling engine

The efficiency of the first order model is equivalent to that obtained by Carnot. In order to be more realistic this efficiency is multiplied by some experience factors. Michels [13] points out that the brake efficiency is in the range of 46-69% of Carnot, while Finegold and Vanderbrug concluded that the max brake efficiency is 52% of Carnot based on the Philips Ford 4-215 engine. Martini [13] indicates that the maximum net brake efficiency is in the range of 38 – 65 % of the Carnot efficiency.

Carlqvist *et al.* [13] give an equation for a well optimised engine using hydrogen as working fluid. In this equation heater efficiency, mechanical efficiency and auxiliary ratio (such as cooling fan, blower, and fuel pump efficiencies) are considered.

The Reitlinger theory gives another equation for calculating the Stirling engine efficiency. This is given in Equation 43. The Reitlinger theory considers also the efficiency of the regenerator, η_r [12].

$$\eta_s = \frac{R\Delta Tln\varepsilon}{T_{max}Rln\varepsilon + (1 - \eta_r)c_v\Delta T} \tag{43}$$

When $\eta_r = 1$, $\eta_s = \eta_c$

Schmidt cycle performance analysis

In this study a numerical and analytical Schimdt cycle analysis was carried out for a gamma type engine with a fixed dead volume.

Figure 5, Figure 6 and Figure 7 shows the work done per cycle at a temperature difference of 250°C, and at a fixed stroke of 24mm for three different phase angles i.e. 75°, 90° and 105° respectively plotted against different diameter ratios, D_D/D_p. Note that the graphs are given for power piston diameter of 60, 80, 100, 150 and 200mm. From these graphs it can be noticed that when the power piston diameter increases the work output also increases, this is due to more swept volume. The work output per cycle for a fixed power piston diameter, D_p, also increases as the ratio of the pistons (D_D/D_p) increases. But this is not as effective as increasing the power piston diameter. This gain is shown as a percentage in Table 2. One can note that the higher the temperature difference the higher this percentage increase in work. Additionally the 75° phase angle exhibits the largest percentage gain, which was followed by the 90° (as the piston diameter increases the percentage difference remains nearly the same). Furthermore, the increase in the work per cycle with respect to the diameter ratio is followed with a decrease in efficiency since the compression ratio is reduced (Figure 11)
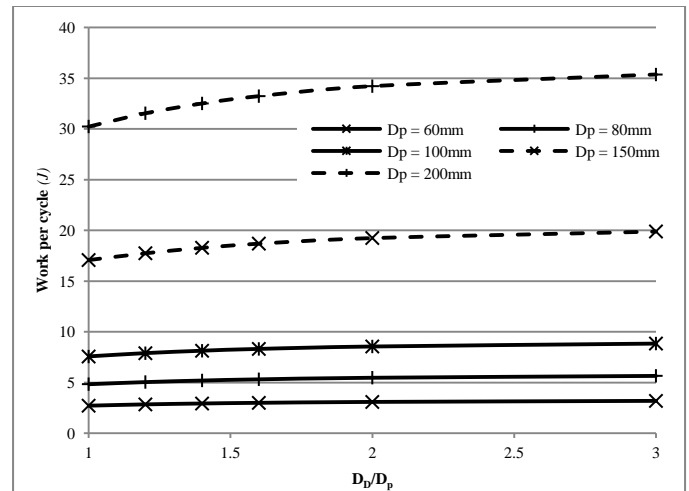
Figure 5 Work done per cycle against diameter ratio at $\Delta T = 250°C$ ($T_c = 50°C$), **α = 75°** and stroke = 24mm
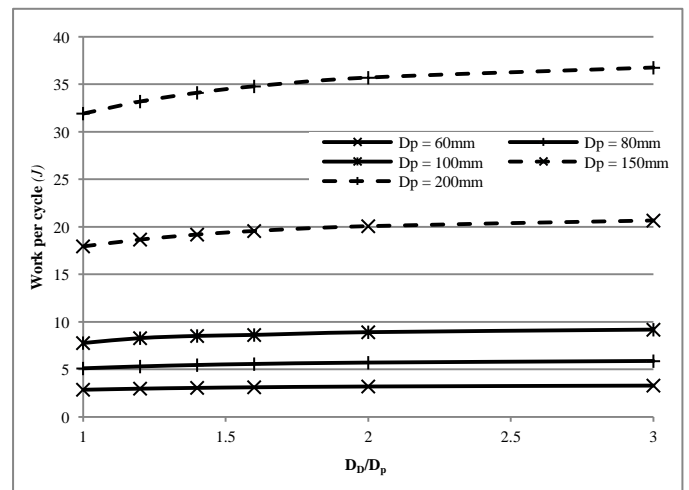
Figure 6 Work done per cycle against diameter ratio at $\Delta T = 250°C$ ($T_c = 50°C$), **α = 90°** and stroke = 24mm
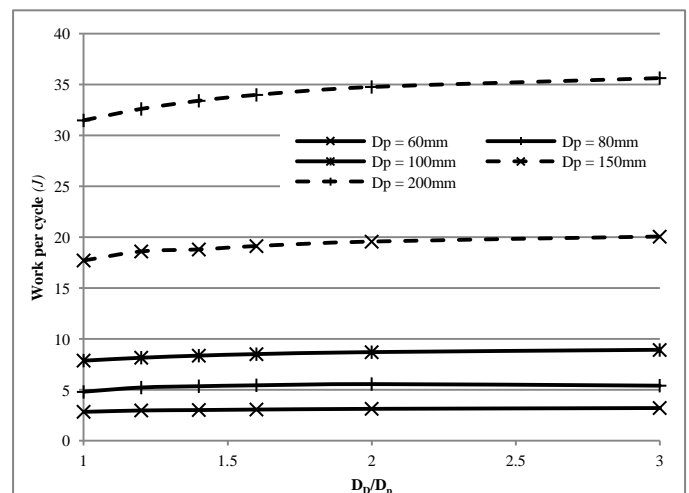
Figure 7 Work done per cycle against diameter ratio at $\Delta T = 250°C$ ($T_c = 50°C$), **α = 105°** and stroke = 24mm

Table 2 Percentage gain in work output from diameter ratio (D_D/D_p) of 1 to 3.

| % increase in work output from a ratio (D_D/D_p) of 1 to the ratio of 3 at D_p=60mm and at 24mm stroke for different phase angles			Temperature difference, °C
75°	90°	105°	
14.8	**13.1**	**11.7**	**250**
19.4	17.6	15.6	400
22.0	19.9	17.7	500
24.2	22.0	19.6	600

Considering a case study:

If the required operating temperature of an engine is 300°C and assuming a 50°C cold sink i.e. 250°C temperature difference, the compression ratio (i.e. excluding the dead volume) according to the empirical formula (Equation 7) shall be 1.23. If the stroke of the displacer and power piston is equal to 24mm, the ratio D_D/D_p should be equal to 2.1 (using Equation 6), (Including the calculated dead volume in D_D/D_p =1.8)

This compression ratio (ε=1.23) and temperature difference gives an efficiency of nearly 7% calculated using the Retilinger equation with no regenerator. Note that the Carnot efficiency for a temperature difference of 250°C is 43.6%.

From Figure 6 for a 60 mm power piston diameter at 90° phase angle at 24mm stroke, the work per cycle is 3.18J for D_D/D_p =1.8 and 3.23J for D_D/D_p =2.1.

Figure 8, Figure 9 and Figure 10 illustrates the work per cycle against the diameter ratio (D_D/D_p) at phase angles of 75°, 90° and 105° respectively at a fixed D_p=60mm and fixed stroke = 24mm for varies temperature difference. It shows that the higher the temperature difference the higher is the work output. From these graphs it can be noticed that when having an already constructed engine say having ε=1.23 i.e. should operate at low temperature difference, if a higher temperature at the heat source is available, the engine would have the potential to produce more work output.
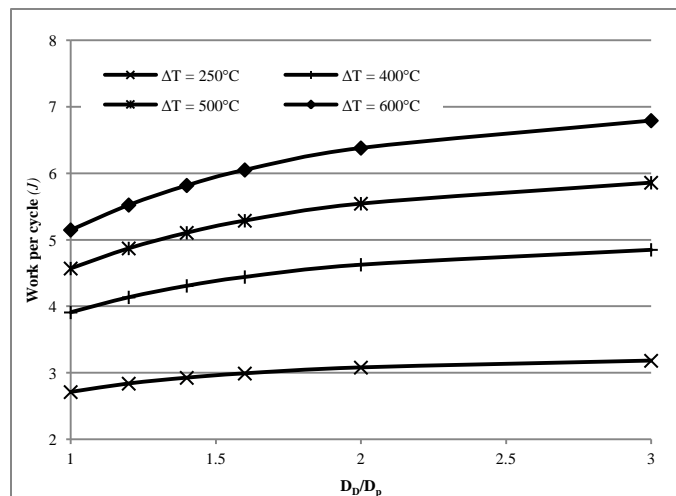
Figure 8 Work per cycle against diameter ratio at **α = 75°** and stroke = 24mm for various ΔT (250°C, 400°C, 500°C, 600°C) (T_c = 50°C)
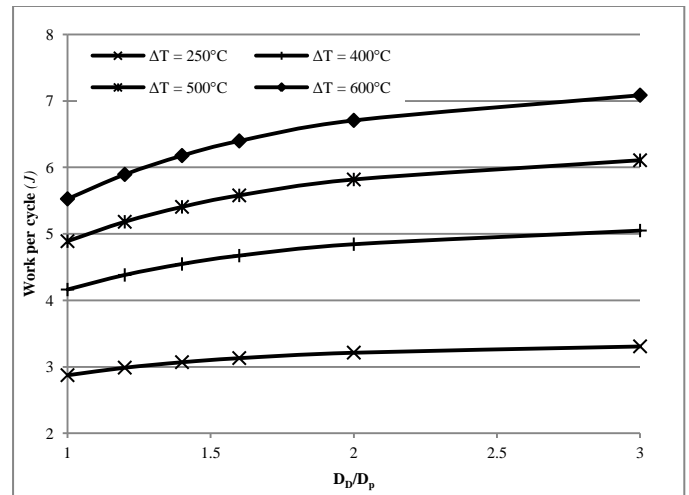
Figure 9 Work per cycle against diameter ratio at **α = 90°** and stroke = 24mm for various ΔT (250°C, 400°C, 500°C, 600°C) (T_c = 50°C)
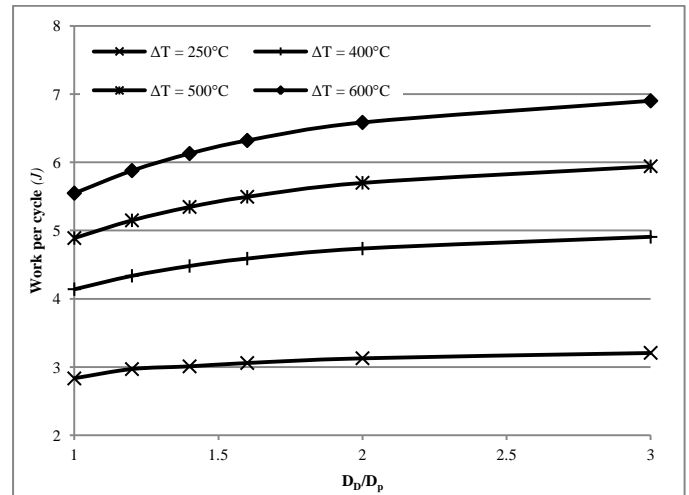
Figure 10 Work per cycle against diameter ratio at **α = 105°** and stroke = 24mm for various ΔT (250°C, 400°C, 500°C, 600°C) (T_c = 50°C)

The percentage increase in work output for an increase in temperature difference at the considered case study (i.e. D_D/D_p= 2.1 at 90° phase angle at 24mm stroke) is shown in Table 3

Table 3 Percentage increase in work output w.r.t. temperature difference

% increase in Work output	Temperature difference, °C
33.7% - (3.2134 to 4.845)	250 to 400
16.7 % - (4.845 to 5.818)	400 to 500
13.3% - (5.818 to 6.7089)	500 to 600

Figure 11 show the variation of the Reitlinger efficiency with no regenerator plotted against the diameter ratio at different temperature difference. One can notice that the efficiency is more dependent on the diameter ratio, hence the compression ratio rather than the actual operating temperature difference. When increasing the operating temperature one can expect an increase in work output but not an increase of the same magnitude in efficiency especially when having large diameter ratios (D_D/D_p). Note that the operating temperature for the case study was 300°C at ΔT of 250°C. (Excluding the use of the regenerator)
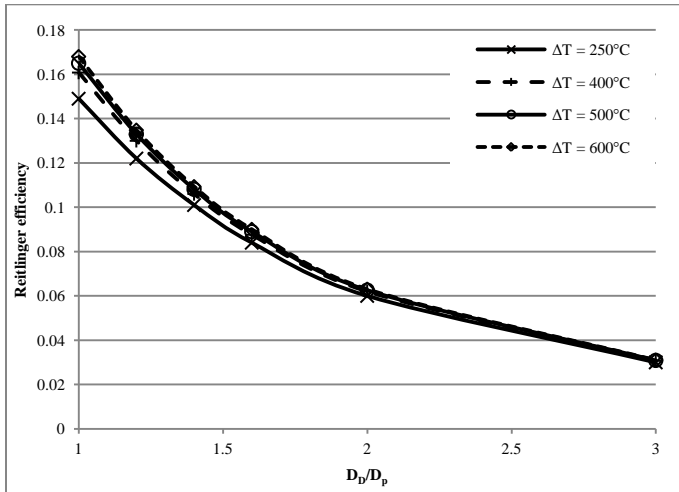
Figure 11 Reitlinger efficiency with no regenerator against diameter ratio ($D_D/D_{p)}$ at varies temperature difference

Analysis limitations

Limitations of such analysis are, that the heat exchangers were assumed to be isothermal whereas in reality they are more adiabatic. The losses such as fluid friction loss, mechanical losses, pressure drops, reheat loss and heat transfer are not considered. This means the output power/work are only a function of the volume, pressure and temperature difference.

Engine power control

In order to keep the optimum power output from an engine it should have some type of power control, these may be [13]:
   a) Increasing dead volume.
   b) Varying the displacer/piston stroke.
   c) Adding or removing working gas.
   d) Changing the phase angle.
   e) Temporary connecting the working space to a buffer space.
   f) Varying the mean pressure within the expansion and compression space by varying the mass of the working fluid.
   g) Increasing/decreasing the amount of heat input.

PARABOLIC TROUGH AND HEAT TRANSFER FLUID CHALLENGES

Market availability

The solar energy collector plays an important part in the micro scale concentrated solar power system. During this study, surveys regarding the availability of parabolic troughs

for domestic purposes (aperture diameter less than 1.6m) indicate only a couple of companies that can supply such collectors.

To the authors best knowledge; the companies that can supply these parabolic troughs are Sopogy [16] and I.T collect [17]. Sopogy produces three different troughs, the Sopoflare which operates at a temperature of 121°C (aperture 0.76m), Soponova which operates at 270°C (aperture 1.65m) and Sopohelios which operates at 326°C (aperture 2.09m). While I.T Collect produce a smaller scale trough operating at 250°C (aperture 0.5m). Both companies include single axis tracking in their product.

A fundamental element of a parabolic trough system is the heat transfer fluid. When it flows through the receiver it absorbs the solar thermal energy concentrated by the collector. The fluid has an important role in a system because it determines important parameters such as operating temperature and the thermal storage technology that can be implemented.

Heat transfer fluid for concentrating solar power can be categorised as follows (Figure 12, [18])**:**
   1.   Synthetic oil
   2.   Traditional salt
   3.   Advanced Heat transfer fluid (HTF)
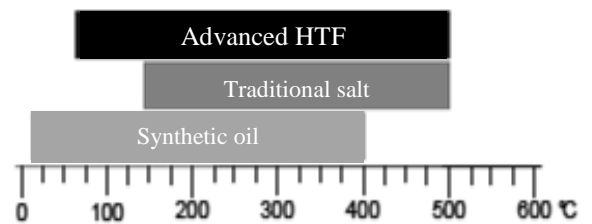
Figure 12 Heat transfer fluid categories with respect to their operating temperature [18]

The most popular heat transfer fluid that is being used in concentrating solar power plants is synthetic oil. This high temperature oil is an organic substance consisting of a eutectic mixture of Biphenyl ($C_{12}H_{10}$ 26.5%) and Diphenyl oxide ($C_{12}H_{10}O$ 73.5%) having an operating temperature range between 12°C and 390°C. Two major companies that develop this type of heat transfer fluid are Soltuia Theminol and DOW under the trade names of VP-1 and Dowtherma-A respectively [19], [20]**.** The main limitations of such fluid are the cost, the operating temperature range and the relatively high vapour pressure. The latter limitation restricts the possibility for thermal storage medium because it will require special designed pressure vessels. A brief list of properties with respect to the mentioned brand names is found in Table 4.

Another category of heat transfer fluid is the traditional molten salts which are commercially available under the brand Hitec [18]. The constituents of molten salts are a binary and also a ternary mixture of nitrates (NO_3) or/and nitrites (NO_2). Three types of molten salts are:
   i.   Solar salt (60%$NaNO_3$,40%KNO_3),
   ii.   Hitec (7%$NaNO_3$,53%KNO_3, 40%$NaNO_2$) and
   iii.   Hitec XL (7%$NaNO_3$,45%KNO_3, 48%$Ca(NO_3)_2$)

The three salts mentioned above exhibits many desirable heat transfer quantities at high temperature. They have high density, high heat capacity, high thermal stability, very low vapour pressure (ease of thermal storage) and low viscosity (low enough for sufficient pumpability) [18]. Additionally they are less expensive, non flammable and more environmental friendly when compared to the synthetic oil.

A drawback of such heat transfer fluid is their high freezing point which is typically in the range of 120-220°C (melting 240°C) depending on the mixture [18]. This limit leads to additional expenses such as, anti-freeze system and thicker insulation. Moreover the fact of having a higher operating temperature implies an extra expense in specific materials, although it results in higher conversion efficiency [21]

A patent for an advanced heat transfer fluid was made by Raade and Padowitz [18]. They developed a fluid with a low melting point of 65°C and a thermal stability to at least 500°C. Furthermore Ionic liquid is being studied as another potential candidate in advance heat transfer fluid.

A comparison of synthetic oil (VP-1), molten salts and Ionic liquid (omimBG4) [21] is illustrated in Table 4.

Table 4 Properties of synthetic oil, molten salts and Ionic liquid **[18] [22] [23]**

Property		Solar salt	Hitec	Hitec XL	LiNO$_3$ mixture	Therminol VP-1	Ionic liquid
Composition%	**NaNO$_3$**	60	7	7	x	Biphenyl and Diphenyl oxide	---
	KNO$_3$	40	53	45	x		---
	NaNO$_2$		40		---		---
	Ca(NO$_3$)$_2$	---	---	48	x		---
Freezing point (°C)		220	142	120	120	13	<25
Upper temperature (°C)		600	535	500	550	400	400
Density @ 300°C,kg/m^3		1889	1640	1992	---	815	1400(@25)
Viscosity @ 300°C,cp		3.26	3.16	6.37	---	0.2	---
Heat capacity @ 300°C,J/kg-K		1495	1560	1447	---	2319	2500 (25)
Cost per kg ($/kg)		0.49	0.93	1.19	---	2.2	---
Manufacturer		Coastal chemical	Coastal chemical	Coastal chemical	---	Solutia/Dow chemical	---

Introducing thermal energy storage in a system is not a new concept, but if a system is utilizing synthetic oil, at an elevated temperature it exhibits high vapour pressure. Thus, a pressure vessel would be required; this may be feasible for a domestic purpose system since the vessel capacity do not need to be too large as the case for Megawatt-scale plants. Furthermore the purpose of the storage tank is more to cover periods of indirect sunlight rather than to operate during sunset hours.

On the other hand, although molten salts have a negligible vapour pressure, they have a high freezing point which would add to the complexity of the plant, such complexities include auxiliary heaters in the system.

CONCLUSIONS

The study reveals that developing a micro scale concentrated solar power system utilising a Stirling engine as the prime mover for electricity production offers a number of challenges. These challenges include the design of a low/medium temperature engine in order to match the power output to the available temperature source, the limited availability of solar energy collector that can deliver heat to the engine by means of a heat transfer fluid at a temperature of at least 400°C and the feasibility of a thermal storage system to cover periods of low solar radiation levels.

REFERENCES

[1] D.Thimsen, "Stirling Engine Assessment," Energy International, Inc., Bellevue, Technical Report 2002.

[2] (2011, September) Genoastirling. [Online]. www.genoastirling.com

[3] SunPower. (2012, February) SunPower High Performance Free-Piston Stirling Engines. [Online]. www.sunpower.com

[4] (2012, february) Whispergen heat and power systems. [Online]. www.whispergen.com

[5] (2012, February) Infinia. [Online]. www.infiniacorp.com

[6] (2012, February) Microgen engine corporation your personal power plant. [Online]. www.microgen-engine.com

[7] (2012, February) Coolenergy. [Online]. www.coolenergyinc.com

[8] A. McConkey and T.D.Eastop, *Applied Thermodynamics for Engineering Techologists*, 5th ed.: Longman Group, 1993.

[9] I. Urieli and D.M.Berchowitz, *Stirling cycle engine analysis*.: Adam Hilger Ltd, 1982.

[10] Prof.S.L.Bapat, "Stirling Engine," Indian institute of Technology, Bombay, Presentation 2008.

[11] Graham Walker, *Stirling Engines*.: Oxford University Press, 1980.

[12] I. Kolin, *Stirling motor: History - Theory - Practise*.: Dubrovnik University, 1991.

[13] W.R. Martini, *Stirling engine design manual*, 1st ed., 1980.

[14] W.R.Martini, *Stirling Engine Design Manual*, 2nd ed. Washington, 1983.

[15] S.K. Verma D.G. Thombare, "Technological development in the Stirling cycle engines," July 2006.

[16] (2011, September) Sopogy. [Online]. http://www.sopogy.com

[17] (2011, September) IT.Collect. [Online]. http://www.it.collect.de

[18] Justin W.Raada and David Padowitz, "Development of Molten Salt Heat Transfer Fluid with Low Melting Point and High Thermal Stability," California,.

[19] (2012, January) Therminol Heat Transfer Fluid. [Online]. www.therminol.com

[20] (2012, January) DowthermaA. [Online]. www.dow.com

[21] Daniel M.Blake et al., "New Heat Transfer and Storage Fluids for Parabolic Trough Solar Thermal Electrical Plants," 11th SolarPACES International Symposium on Concentrating Solar Power and Chemical Energy Technologies, 2002.

[22] B.Kelly, R.Cable, U.Hermann, R.Mahoney, D.Blake D.Kearney, "Assessment of Molten Salt Heat Transfer Fluid in a Parabolic Trough Solar Field," *JSEE*, April 2002, Copyright by ASME.

[23] D.W. Kearney et al., Engineering Evaluation of a Molten Salt HTF in a Parabolic Trough Solar Field, August 2001, NREL Contract No. NAA-1-30441-04.